Integrated Electricity and Gas Systems Modelling: Assessing the Impacts of Electrification of Residential Heating in Victoria

Isam Saedi
Electrical and Electronic Engineering
The University of Melbourne
Victoria, Australia
isaedi@student.unimelb.edu.au

Sleiman Mhanna
Electrical and Electronic Engineering
The University of Melbourne
Victoria, Australia
sleiman.mhanna@unimelb.edu.au

Han Wang
Electrical and Electronic Engineering
The University of Melbourne
Victoria, Australia
wang.h3@unimelb.edu.au

Pierluigi Mancarella
Electrical and Electronic Engineering
The University of Melbourne
Victoria, Australia
pierluigi.mancarella@unimelb.edu.au

***Abstract*— Electricity and gas systems are undergoing a fast transition towards low-carbon and more integrated energy systems. One of those pathways is the electrification of residential heating, whose impacts can be better quantified by *jointly* modeling the two systems. This paper presents a novel integrated electricity and gas transmission system model with high spatio-temporal resolution and realistic system operating constraints. The electricity system model is a unit commitment with a strengthened DC optimal power flow, formulated as a mixed-integer linear program. The gas network model consists of a dynamic gas flow model that captures gas network flexibility, as measured by the linepack. The model is implemented on projected 2025 case studies with the actual Victorian transmission systems, assuming the use of air-to-water electric heat pumps for both space heating and domestic hot water. In the context of the specific assumptions and scenarios considered, results suggest that: (i) residential electrification will generally require additional imports and/or local generation, and interconnectors and intra-state transmission lines may also need augmentation in scenarios with full electrification; (ii) the gas network can provide the flexibility needed by the system in most electrification cases; and (iii) the total electricity-gas CO_2 emissions might slightly *increase* as electrification increases.**

Keywords*— *Electrification of heating, air-source heat pumps, unit commitment, strengthened DC OPF, dynamic gas flow, low-carbon economy, CO_2 emissions.

I. Introduction

Nowadays, the utilisation of the gas transmission network is generally dominated by gas-powered generators (GPGs) and the heating sector. Moreover, the push towards multi-energy systems [1] to reduce costs and greenhouse gas emissions will also increase the interactions between different energy sectors and vectors. Despite their physical coupling, electricity and gas systems are currently operated, managed, and planned separately. This therefore calls for developing *integrated* modelling frameworks that *jointly* coordinate multiple energy networks [2] to better capture the multi-energy nature, constraints, spatial and temporal inter-dependencies, and synergy opportunities of future systems.

One of the pathways towards low-carbon multi-energy systems is the electrification of residential heating, which consists of shifting (some) heating demand from the gas to the electricity network to reduce carbon emissions as the electricity system gets decarbonised. In a scenario where a country's heat demand is mainly fulfilled by gas, the electrification of the heating sector has been shown to lead to higher electrical demand peaks [3]–[6]. Conversely, the works in [7]–[9] show that the heating sector can offer flexibility to the power system, through demand response or load shifting for instance, and enhance system resilience [10]. Moreover, the work in [11] evaluates the impact of electrifying the heating sector through electric heat pumps (EHP), as opposed to gas-based heating, on the gas generation ramp requirements. On the other hand, the work in [12] uses historical meteorological data to evaluate GPG demand of alternative heating technologies and showcases noticeable changes especially in scenarios with increased solar generation. Additional detailed insights into the impact of low-carbon hybrid heating technologies on the integrated heat, electricity, and gas systems are presented in [13] and [14] for the UK. A study on the full electrification of heating demand for Australia is conducted in [15], but only considers the electricity system and a hypothetical scenario with 100% renewables. However, studies on the implications on the flexibility and adequacy of electricity and gas systems under the electrification of residential heating and within an integrated-system framework are still in their infancy. In fact, this work is the first to assess the impact of residential heating electrification on the adequacy and flexibility of electricity and gas transmission systems using a UC model with a *strengthened* DC-OPF, which incorporates transmission line *losses* and actual technical specifications of individual generating units. More specifically, as losses grow with the square of the electric current, they become more prominent at peak times, which is especially important in the case of heating electrification when heating peak demand compounds the electricity demand in winter. This work is also the first to assess the impact of electrification of residential heating demand on the adequacy, flexibility, and CO_2 emissions of the electricity and gas transmission systems of Victoria.

Against this background, this paper introduces an integrated electricity and gas systems (IEGS) model with relatively high spatiotemporal resolution and suitable operating constraints, and whose capabilities are demonstrated on case studies consisting of electrification of residential heating on the electricity and gas transmission networks of Victoria, Australia for the year 2025. The IEGS framework implements (i) a dynamic gas flow model that is suitable for capturing the flexibility of the gas network, and (ii) a UC model with a strengthened DC-OPF that incorporates transmission line losses, reserve requirements, ramp rates, and minimum up-and-down time constraints on generators. The

This work is supported by Future Fuels CRC as part of the R.P1.1-02: "Regional Case Studies on Multi-Energy System Integration" project. The cash and in-kind support from the industry participants is gratefully acknowledged.

electrification of heating is assumed to be based predominately on air-to-water EHP [16].

The paper is structured as follows. Section II describes the mathematical modelling of the proposed IEGS model. Section III presents the overall modelling methodology. The proposed model is validated in Section IV with case studies involving the Victorian electricity and gas transmission networks. The paper concludes in Section 0.

II. Mathematical Modelling

A. Electricity System Modeling

The electricity system model is a UC model with a "strengthened" DC-OPF solved over a 24-hour scheduling horizon with a half-hourly resolution. The strengthened DC-OPF minimises the overall operational cost while satisfying electricity demand subject to network constraints that include *losses*. As losses grow with the square of the electric current, they become much more significant at peak times, which is particularly important in the case of heating electrification when heating peak demand compounds the electricity demand in winter. UC constraints include minimum stable generation (MW), minimum up-time and down-time (hours), ramp rates (MW/minute), and reserve requirements (MW). These are all obtained from the AEMO [17].

In more detail, let $\mathcal{G}^{\mathrm{C}}, \mathcal{G}^{\mathrm{G}}$, and $\mathcal{G}^{\mathrm{RG}}$ denote the sets of coal, gas, and renewable generators, respectively. The objective function can be mathematically expressed as

$$\text{Min } f(P) = \sum_{t\in\mathcal{T}} \left(\sum_{gm\in\mathcal{G}^{\mathrm{C}}\cup\mathcal{G}^{\mathrm{G}}\cup\mathcal{G}^{\mathrm{RG}}} f_{gm}\left(P_{gm,t}\right) \right), \quad (1)$$

where $P_{gm,t}$ is the real power output of generator gm and f_{gm} is the corresponding cost function. The operational constraints on the electricity system are:

$$\underline{P}_{gm} \le P_{gm,t} \le \overline{P}_{gm}, \quad gm \in \mathcal{G}^{\mathrm{C}} \cup \mathcal{G}^{\mathrm{G}} \cup \mathcal{G}^{\mathrm{RG}}, t \in \mathcal{T} \quad (2)$$

$$-\overline{P}_{mn} \le P_{mn,t} \le \overline{P}_{mn}, \quad mn \in \mathcal{L}, t \in \mathcal{T} \quad (3)$$

$$\underline{\Delta\theta}_{mn} \le \theta_{m,t} - \theta_{n,t} \le \overline{\Delta\theta}_{mn}, \quad mn \in \mathcal{L}, t \in \mathcal{T} \quad (4)$$

$$\sum_{gm\in\mathcal{G}^{\mathrm{C}}} P^{\mathrm{r}}_{gm,t} \ge \mathrm{SR}, \quad t \in \mathcal{T} \quad (5)$$

$$\sum_{g\in\mathcal{G}^{\mathrm{C}}_m\cup\mathcal{G}^{\mathrm{G}}_m\cup\mathcal{G}^{\mathrm{RG}}_m} P_{gm,t} = P^{\mathrm{d}}_{m,t} + \sum_{n\in\mathcal{B}_m} P_{mn,t}, \quad m \in \mathcal{B}, t \in \mathcal{T} \quad (6)$$

$$P_{mn,t} = g_{mn}\, 0.5\left(\theta_{mn,t}\right)^2 + b_{mn}\theta_{mn,t}, \quad mn \in \mathcal{L}, t \in \mathcal{T} \quad (7)$$

$$P_{nm,t} = g_{nm}\, 0.5\left(\theta_{mn,t}\right)^2 - b_{nm}\theta_{mn,t}, \quad nm \in \mathcal{L}^{\mathrm{t}}, t \in \mathcal{T} \quad (8)$$

$$P_{gm,t} + P^{\mathrm{r}}_{gm,t} \le u_{gm,t}\overline{P}_{gm}, \quad gm \in \mathcal{G}^{\mathrm{C}}, t \in \mathcal{T} \quad (9)$$

$$P_{gm,t} \ge u_{gm,t}\underline{P}_{gm}, \quad gm \in \mathcal{G}^{\mathrm{C}}, t \in \mathcal{T} \quad (10)$$

$$P_{gm,t} + P^{\mathrm{r}}_{gm,t} \le \overline{P}_{gm}, \quad gm \in \mathcal{G}^{\mathrm{C}}, t \in \mathcal{T} \quad (11)$$

$$P_{gm,t} - P_{gm,t-1} \le u_{gm,t-1}RU_{gm} + v_{gm,t}\underline{P}_{gm}, \; gm \in \mathcal{G}^{\mathrm{C}}, t \in \mathcal{T} \quad (12)$$

$$P_{gm,t-1} - P_{gm,t} \le u_{gm,t}RD_{gm}, \quad gm \in \mathcal{G}^{\mathrm{C}}, t \in \mathcal{T} \quad (13)$$

$$\sum_{t^{\mathrm{up}}=t-\mathrm{MUT}_{gm}+1} v_{gm,t^{\mathrm{up}}} \le u_{gm,t}, \; gm \in \mathcal{G}^{\mathrm{C}}, t \in \left\{\mathrm{MUT}_{gm},..,\mathcal{T}\right\} \quad (14)$$

$$\sum_{t^{\mathrm{dn}}=t-\mathrm{MDT}_{gm}+1} w_{gm,t^{\mathrm{dn}}} \le 1 - u_{gm,t}, \; gm \in \mathcal{G}^{\mathrm{C}}, t \in \left\{\mathrm{MDT}_{gm},..,\mathcal{T}\right\} \quad (15)$$

$$v_{gm,t} - w_{gm,t} \ge u_{gm,t} - u_{gm,t-1}, \quad gm \in \mathcal{G}^{\mathrm{C}}, t \in \mathcal{T} \quad (16)$$

$$v_{gm,t}, w_{gm,t} \in [0,1], \; u_{gm,t} \in \{0,1\}, \quad gm \in \mathcal{G}^{\mathrm{C}}, t \in \mathcal{T} \quad (17)$$

where $\mathcal{L}$ / $\mathcal{L}^{\mathrm{t}}$ denote the set of all branches *mn/nm* where *m/n* are the from/to buses. The set of buses is denoted by $\mathcal{B}$. Parameters $\underline{P}_{gm,t}$ and $\overline{P}_{gm,t}$ are the minimum and maximum power of each unit [MW], respectively, $\underline{\Delta\theta}_{mn}$ and $\overline{\Delta\theta}_{mn}$ are the minimum and maximum angle difference between buses *m* and *n*, RU_{gm} and RD_{gm} are the up and down ramp rates of each unit [MW/h], SR is the spinning reserve, $P^{\mathrm{d}}_{m,t}$ is the real power demand [MW], g_{mn} is the line conductance [pu], b_{mn} is the line susceptance [pu], and MUT_{gm}/MDT_{gm} denote the generator minimum up/down time [h]. Variables $P_{mn,t}$ and $\theta_{mn,t}$ are the power flow through line *mn* [MW] and the angle difference between buses *m* and *n* [rad], respectively, and $P^{\mathrm{r}}_{gm,t}$ is the spinning reserve (assumed to be provided by coal-fired generators, aligned with current practices) [MW]. Binary variable $u_{gm,t}$ represents generator on or off status, and is equal to 1 if unit *gm* is on, and 0 otherwise. Variable $v_{gm,t}$ represents the generator start-up, and is equal to 1 only at the start-up of unit *gm*, and 0 otherwise. Analogously, $w_{gm,t}$ represents the generator shut-down, and is equal to 1 only when unit *gm* is shut down, and 0 otherwise.

The limits on active power output from each generator are captured by (2). The limits on transmission line active power and angle difference are captured by (3) and (4), respectively. The spinning reserve requirement is given in (5). Kirchhoff's current law (KCL) is satisfied through (6). The real power flow constraints are given in (7) and (8) in which the line losses are approximated using the second-order Maclaurin series of the cosine function in the original AC OPF formulation, i.e, $\cos(\theta_{mn}) \approx 1–0.5(\theta_{mn})^2$. The ensuing nonlinear and nonconvex constraint is then approximated using piecewise linear segments.

The UC constraints are delineated by (9)–(17), where (9)–(11) capture the limits on active power, whereas (12) and (13) capture the ramping capabilities of a coal generator. The minimum up-time and minimum down-time of a generating unit are captured by (14) and (15). More interestingly, because $u_{gm,t}$ is binary, variables $v_{gm,t}$ and $w_{gm,t}$ can be modelled as continuous (as opposed to binary) thanks to constraint (16) which ensures that they take binary values in the solution. In fact, if (16) is used to pivot $w_{gm,t}$ out of the system given by (14) and (15), the resulting set defines the convex hull of the minimum up-time and down-time polytope on the space of variables $u_{gm,t}$ and $v_{gm,t}$. Finally, the integrality constraint on the $u_{gm,t}$ variables is described by (17). The resulting model is a MILP that can be solved efficiently using state-of-the-art industrial solvers.

B. Gas System Model

The gas system model consists of a dynamic optimal gas flow formulation that can predict the network operating conditions over the 24-hour scheduling horizon. The importance of transient gas-flow modelling becomes salient in gas transmission networks where supply and demand are frequently changing states. Because the gas system is characterized by slow dynamics, the fluctuations in gas demand are not balanced instantaneously. These mismatches are usually buffered by the linepack which represents the volume of pressurized gas stored in a pipeline.

The transient behaviour of an isothermal gas flowing in a horizontal pipeline is delineated by the continuity equation and the motion equation [18]. These can be described by

$$\frac{\rho_n RT}{A_{ij}} \cdot \frac{\Delta t}{\Delta x}\left(q_{ij,t}^{\text{out}} - q_{ij,t}^{\text{in}}\right) + \frac{p_{ij,t}^{\text{av}}}{Z_{ij,t}} - \frac{p_{ij,t-1}^{\text{av}}}{Z_{ij,t-1}} = 0, \quad (18)$$

$$\frac{p_{j,t}^2 - p_{i,t}^2}{\Delta x} + \frac{\left(q_{ij,t}^{\text{out}} + q_{ij,t}^{\text{in}}\right) \cdot \left|q_{ij,t}^{\text{out}} + q_{ij,t}^{\text{in}}\right| \rho_n^2 Z_{ij,t} RT f_{ij}}{4 D_{ij} A_{ij}^2} = 0, \quad (19)$$

where $q_{ij,t}^{\text{in/out}}$ is the inlet/outlet volumetric gas flow rate through the pipeline ij [m^3/s], ρ_n is the gas density at standard conditions (i.e., p_n = 101325 Pa and T_n = 288.15 K) [kg.m^{-3}], R is the specific gas constant [J kg^{-1} K^{-1}], T is the gas temperature [K], $Z_{ij,t}$ is the compressibility factor [-], $p_{ij,t}^{\text{av}}$ is the average gas pressure [Pa], A_{ij} is the pipeline cross-sectional area [m^2], $p_{i,t}$ is the gas pressure at node i [Pa], f_{ij} is the friction factor [-], D_{ij} is the pipeline diameter [m], Δt is the time resolution [s], and Δx is the pipeline spatial coordinate [m].

The compressibility and friction factors are expressed as

$$Z_{ij,t} = \frac{1}{1 + \frac{49.9511 p_{ij,t}^{\text{av}} \times 10^{1.785S}}{(T * 1.8)^{3.825}}}, \quad (20)$$

$$f_{ij} = 4\left(20.621 \eta_{ij} (D_{ij})^{1/6}\right)^{-2}, \quad (21)$$

respectively, where S is the gas relative density [-] [19].

If $\mathcal{N}$ is the set of gas nodes, $\mathcal{S}$ is the set of gas suppliers, and $\mathcal{E}$ is a set of all edges in the gas system, then the mass conservation at node i can be written as

$$\sum_{s \in S_i} q_{si,t}^{\text{S}} + \sum_{ji \in \mathcal{E}} q_{ji,t} - \sum_{ij \in \mathcal{E}} q_{ij,t} = q_{i,t}^{\text{D}}, \quad i \in \mathcal{N} \quad (22)$$

where $q_{si,t}^{\text{S}}$ is the gas supply flow rate [m^3/s] and $q_{i,t}^{\text{D}}$ is the gas demand flow rate [m^3/s].

Finally, the linepack in a pipeline can be described by

$$Lp_{ij,t} = V_P \frac{p_{ij,t}^{\text{av}}}{\rho_n Z_{ij,t} RT}, \quad (23)$$

where $Lp_{ij,t}$ is the linepack [m^3], and V_p is the pipeline physical volume [m^3].

C. Electrification of Heating Methodology

This section describes the methodology underlying the modelling of both space heating (SH) and domestic hot water (DHW) demands in the state of Victoria. Residential gas demand profiles used in this study are based on the analysis in [20] and the assumptions in [21] and [22]. In more detail, gas-based SH and DHW demands are assumed to account for 75% and 23% of the residential gas consumption, respectively, whereas cooking demand accounts for 2% of the residential gas consumption and is assumed to be uniform between 5PM and 11PM [21], [22]. The normalized residential gas demand profile for a typical winter weekday is depicted in Fig. 1.The proportions of gas consumption in different sectors, excluding the gas consumed by GPGs, are 49%, 16%, and 35% for residential, commercial, and industrial sectors, respectively [22], [23].

Existing gas DHW and electric hot water heaters are assumed to have average thermal efficiencies of 85% and 95%, respectively [24], [25]. Air-to-water EHP technology is assumed here for both SH and DHW with a coefficient of performance (CoP) shown in Fig. 2 for different water temperatures ranging from 30°C to 55°C. The CoP of EHP varies with respect to outside temperature and the heating

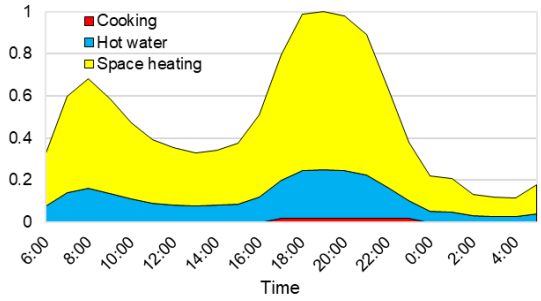

Fig. 1. Normalized residential gas demand profile for a typical winter weekday.

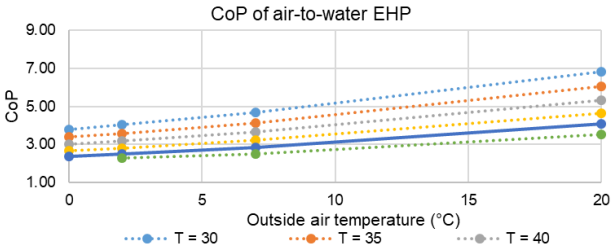

Fig. 2. CoP of air-to-water EHP for different water temperatures ranging from 30°C to 55°C.

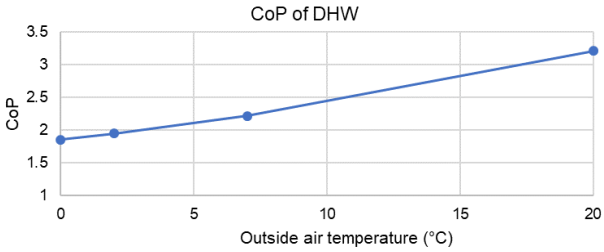

Fig. 3. Overall CoP of DHW (air-to-water EHP + electric hot water heater).

system water temperature. The water temperature of the EHP is assumed to be 50°C in all the electrification scenarios below. Electric SH demand is assumed to be provided by EHP with the CoP shown in Fig. 2 for a water temperature of 50°C.

On the other hand, electric DHW demand is assumed to be provided by EHPs *coupled* with electric hot water heaters, for an overall CoP shown in Fig. 3. The hot water heaters, which are assumed to have an efficiency of 95%, are used to raise the water temperature from 50°C to 60°C to prevent the growth of some strains of bacteria (such as Legionella) [26].

Outside temperature profiles for each demand zone are obtained from the Bureau of Meteorology [27] in a half-hourly resolution. Zonal gas demands are obtained from AEMO [28], under "Public D+3 Metering Data". Note that these zonal demands include the gas consumed by GPGs, which were then subtracted with the help of the metered power (MW) outputs obtained from AEMO's SCADA values [29] of the corresponding GPGs. Heat rates (GJ/MWh) of the corresponding GPGs are obtained from [17].

III. Modelling Methodology

The overall modelling methodology is depicted in Fig. 4 The input data consists mainly of the electricity and gas network infrastructures, electricity and gas demand profiles, forecasts of renewable energy sources (RES), generation information, and gas supply information. Demand forecasts and RES availability forecasts are acquired from AEMO [30].

The first stage is the half-hourly UC with strengthened DC-OPF model which determines the optimal dispatch of the

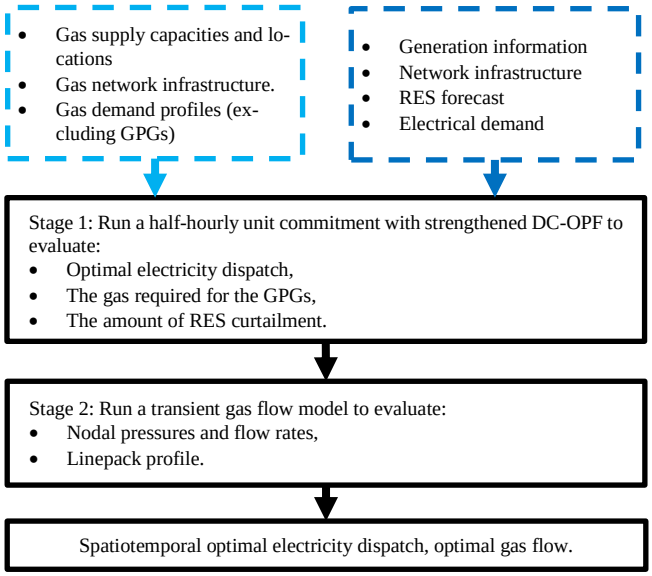

Fig. 4. The overall modelling methodology.

generation mix and the amount, time, and location of RES curtailments. The second stage consists of the transient gas flow model solved over 24 hours with hourly time resolution. The second stage determines the linepack profile, the nodal pressures, and the gas flow rates. The linepack is instrumental in assessing gas network flexibility, which is key in studying the impact of shifting the heating gas demand from the gas to the electricity system, as will be demonstrated below.

IV. Numerical Analysis

The electrification studies in this section are all implemented on the real electricity and gas transmission networks of the state of Victoria, under the "Central" scenario of AEMO's integrated system plan (ISP) [31], for representative winter and autumn days of 2025. The generation mix of 2025 is updated accordingly to include the generation outlook of the renewable energy zones (REZ), obtained from [32], and the retirement plans of some coal-fired generators and GPGs, obtained from [17]. The interconnectors are also augmented accordingly for 2025, as described in [17]. In compliance with [32], the total installed wind and solar capacities in 2025 are 4150 MW and 1357 MW, respectively, for the Central scenario. Finally, Western Victoria's electricity network is augmented as per the preferred option identified in [33]. The gas network model is also augmented to reflect the forecast reduction in gas supply in 2025 and the augmentations of the South West Pipeline (SWP). The studies consist of five different electrification cases in 2025, namely, (i) 1-in-20-year peak gas system demand day, and (ii) low-wind 1-in-20-year peak gas system demand day, (iii) average winter gas demand day, (iv) low-wind average winter gas demand day, and (v) average autumn gas demand day. Each one of the five different electrification scenarios consists of three subcases where gas SH and gas DHW are replaced with electric options: (i) 0% SH and 0% DHW, (ii) 50% SH and 50% DHW, and (iii) 100% SH and 100% DHW. For the purpose of succinctness, only the first case is detailed in this section. Finally, an assessment of CO_2 emissions is conducted on the above set of scenarios, and is detailed in Section IV.B.

A. *1-in-20-year Peak Gas System Demand Day*

In this scenario, the 1-in-20-year peak gas system demand day of August 09, 2019 is projected onto the same day in 2025. The purpose of this scenario is to assess the impact of the electrification of residential heating on both the supply adequacy of both the electricity and gas systems for a 1-in-20-year peak gas system demand day under the generation mix, electricity demand forecasts, and RES output forecasts of August 09, 2025 in the Central scenario of the ISP.

1) 0% SH and 0% DHW (base case)

This base-case scenario is characterized by an average of 1777 MW of wind power and a net gas demand (excluding gas consumed by GPGs) of 1188 TJ/d. The electricity generation profile is shown in Fig. 5. Since there are no imports from other states, it can be concluded that the generation is adequate to supply the demand. Regarding the gas network, the total gas demand (including gas consumed by GPGs) is 1229 TJ/d. The total gas supply capacity available to supply the Victorian gas demand is 1187 TJ/d. The hourly linepack profile, along with the demand and supply profiles for this scenario, are shown in Fig. 6, which also shows a gas supply shortfall equal to 1229 – 1187 = 42 TJ/d. This translates to an end-of-day (EoD) linepack that is 46 TJ below the beginning-of-day (BoD) linepack target, confirming the "stretch" of the gas network under extreme conditions.[1]

2) 50% SH and 50% DHW

This scenario is characterized by an average of 1781 MW of wind power and a net gas demand (excluding gas consumed by GPGs) of 902 TJ/d. Compared to the base case, 286 TJ/d of energy from residential heating is shifted from the gas system to the electricity system. As a result, the electricity generation profile in Fig. 7 shows that the shortfall in generation between 4:30PM to 10PM needs to be supplemented by imports from other states through the interconnectors. However, those imports are within the interconnector capacities and therefore no augmentation is needed. On the gas network side, the total gas demand (including gas consumed by GPGs) is 1117 TJ/d. The hourly linepack profile, along with the demand and supply profiles for this scenario, are shown in Fig. 8, which also shows that the gas supply is adequate, as evidenced by an EoD linepack that is close to the BoD linepack target. This is a desirable outcome as market operators such as AEMO set a BoD linepack target that maintains efficient and safe system operational conditions [34]. The BoD linepack target for the DTS is around 850 TJ in winter and includes both passive and active linepack [35]. The value of the linepack target is set to account for the impact of unscheduled GPG demand and surprise cold weather[2] [35]. Compared to the base case, the GPG demand increased by 174 TJ/d (from 41 TJ/d to 215 TJ/d) but this increase in GPG demand is offset by a larger decrease in residential heating demand for a total gas demand decrease of 112 TJ/d.

3) 100% SH and 100% DHW

This scenario is characterized by an average of 1806 MW of wind power and a net gas demand (excluding gas consumed

[1] The EoD linepack is measured at the end of a gas day at 6AM and is equal to the BoD linepack for the next gas day.
[2] The The linepack is depleted quicker than expected if scheduled BoD injections are lower than required to meet the actual demand (i.e., when actual demand exceeds forecast demand).

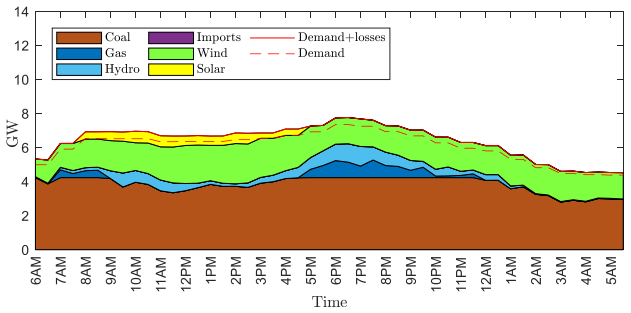

Fig. 5. Generation profile under 0% SH and 0% DHW electrification for the 1-in-20-year peak gas system demand day projected onto August 09, 2025.

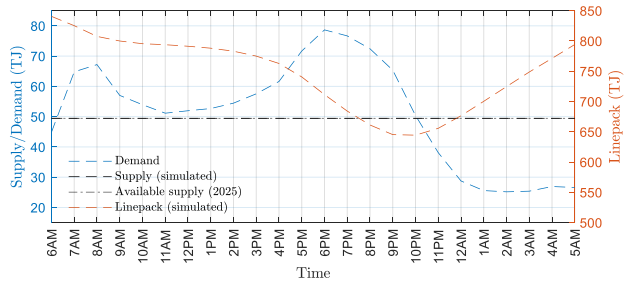

Fig. 6. Linepack and gas supply profiles under 0% SH and 0% DHW electrification, 1-in-20-year gas system demand day projected onto August 09, 2025.

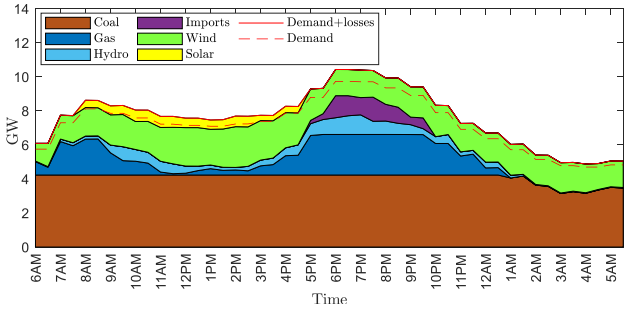

Fig. 7. Generation profile under 50% SH and 50% DHW electrification, for the 1-in-20-year peak gas system demand day projected onto August 09, 2025.

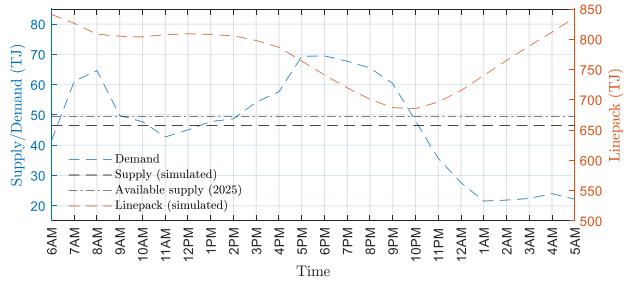

Fig. 8. Linepack and gas supply profiles under 50% SH and 50% DHW electrification, 1-in-20-year gas system demand day projected onto August 09, 2025.

by GPGs) of 615 TJ/d. Compared to the base case, 573 TJ/d of energy from residential heating is shifted from the gas system to the electricity system. As a result, the electricity generation profile in Fig. 9 shows that the shortfall in generation between 6:30AM and 9:30AM and between 4PM to 11PM needs to be supplemented by imports from other states. In this instance, these imports exceed interconnector capacities by an average of 1500 MW, so that interconnector augmentation might be needed. Furthermore, this high demand, which peaks at 12GW, requires network augmentation in the form of an 11% increase in MVA (thermal) capacity on some internal transmission lines. On the gas network side, the total gas demand (including gas consumed by GPGs) is 938 TJ/d. The hourly linepack profile, along with the demand and supply profiles for this scenario,

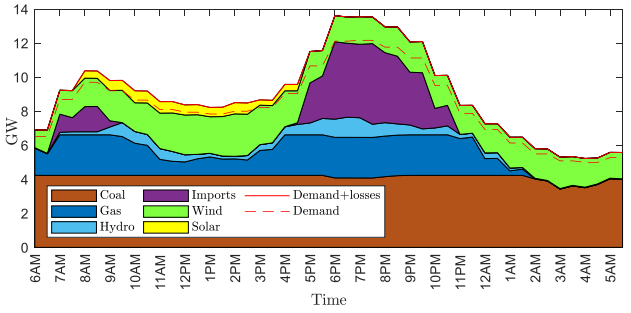

Fig. 9. Generation profile under 100% SH and 100% DHW electrification for the 1-in-20-year peak gas system demand projected onto August 09, 2025.

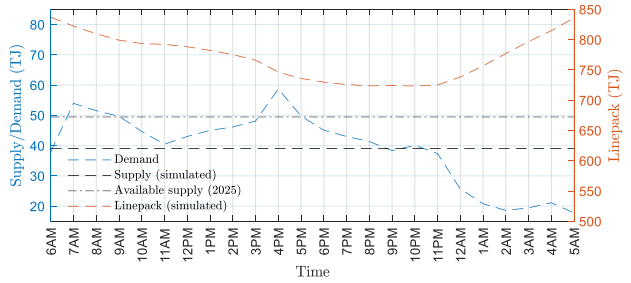

Fig. 10. Linepack and gas supply profiles under 100% SH-100% DHW electrification, 1-in-20-year peak gas system demand projected onto August 09, 2025.

are shown in Fig. 10, which also shows that the gas supply is adequate, as evidenced by an EoD linepack that is close to the BoD linepack target. Compared to the base case, the GPG demand increased by 282 TJ/d (from 41 TJ/d to 323 TJ/d), but this increase in GPG demand is offset by a larger decrease in residential heating demand for a total gas demand decrease of 291 TJ/d compared to the base case.

B. CO_2 Emissions Assessment

The CO_2 emissions for the five electrification cases are shown in Fig. 11. The CO_2 emission factors of coal-fired generators and GPGs range from 1141 to 1315 kg/MWh and from 565 to 880 kg/MWh, respectively [17]. Moreover, the CO_2 emission factor of energy imports are assumed to be 464 kg/MWh to reflect the average emissions factors of the generation mix of 2025 NEM-wide. The CO_2 emissions of NG are taken as 51.4 kg/GJ. It can be observed from Fig. 11 that the CO_2 emissions of the Victorian electricity and gas systems slightly increase with the level of electrification, with decrease in emissions on the gas network side being offset by a larger increase in emissions on the electricity side. The exact numbers depend on the level of RES injections, the synchronous generation mix (coal-fired and gas-powered generators), demand levels, and the topologies of both electricity and the gas networks. Hence, although the generation mix of 2025 includes a large share of RES capacity, shifting a large portion of heating demand from the gas system to the electricity system might actually lead to more CO_2 emissions, differently from what one could expect. This is also partially due to curtailment of energy from RES due to a combination of transmission line thermal constraints and system operating constraints (e.g., reserve requirements), which lead to more dispatch from coal-fired and gas generators, thereby increasing emissions. Furthermore, system losses also increase with higher electrical peaks, and more peaking plants operation is needed too, again leading to emission increase.

V. Conclusion

This paper presented a novel IEGS modelling tool whose demonstrated on transmission system studies for electrification of residential heating for the state of Victoria in

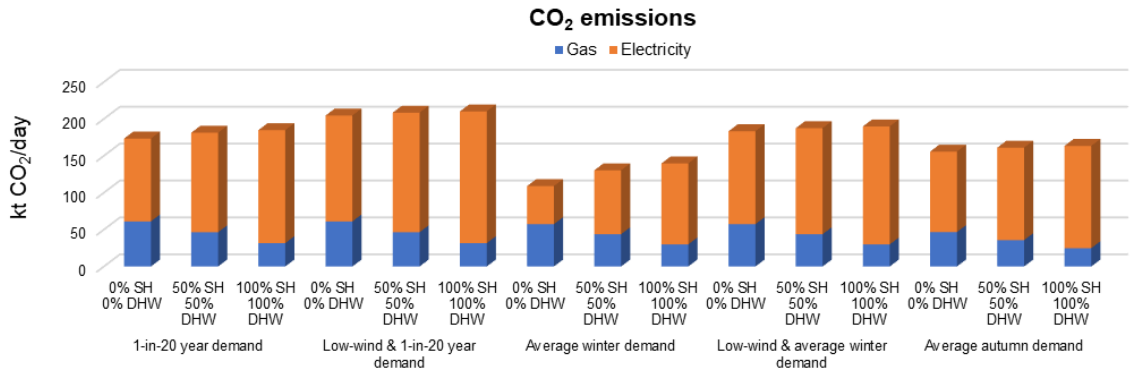

Fig. 11. CO_2 emissions for the five electrification cases.

2025. Key features of the tool are (i) a UC model with a strengthened DC-OPF that incorporates transmission line losses (particularly useful when assessing increasing peak demand) and technical constraints on generators, and (ii) a dynamic gas flow model that is suitable for capturing the flexibility and supply adequacy of the gas network. This work underscores the importance of bottom-up integrated multi-energy sector, network, and system assessment with high spatial and temporal resolution and suitable operating constraints. In more detail, the tool is capable of: (i) assessing the requirements for additional imports or local generation as well as for intra-state network augmentation, for different levels of electrification up to 100% SH and 100% DHW; (ii) predicting the adequacy of gas supply by quantifying the effect of the increase in GPG demand, as a result of electrification, on the gas network flexibility; and (iii) assessing the impact of electrification of heating on the CO_2 emissions of both networks. The results for the Victorian system based on the 2025 scenarios considered suggest that additional *local* generation and/or imports from other states may be needed in most electrification cases, while interconnectors and some internal transmission lines may also require augmentation when the heating demand is fully electrified. On the other hand, the Victorian gas supply is likely to be able to provide the required flexibility in most electrification scenarios, even in the case of increasing GPG peaking operation. Our findings also suggest that the total CO_2 emissions might slightly increase with the electrification, including due to renewable curtailment and as a result of increasing losses and peaking plant operation. However, these findings should be considered in the context of the specific assumptions made, and more studies, also based on alternative scenario and technology sensitivities for electrification of heating, are ongoing.

VI. References

[1] P. Mancarella, "MES (multi-energy systems): An overview of concepts and evaluation models," *Energy*, vol. 65, pp. 1–17, 2014.

[2] G. Andersson and M. Geidl, "Optimal Power Flow of Multiple Energy Carriers," *IEEE Trans. Power Syst.*, vol. 22, no. 1, pp. 145–155, 2007.

[3] I. A. G. Wilson, A. J. R. Rennie, Y. Ding, P. C. Eames, P. J. Hall, and N. J. Kelly, "Historical daily gas and electrical energy flows through Great Britain's transmission networks and the decarbonisation of domestic heat," *Energy Policy*, vol. 61, pp. 301–305, 2013.

[4] P. J. Baruah *et al.*, "Energy system impacts from heat and transport electrification," *Proc. Inst. Civ. Eng. - Energy*, vol. 167, no. 3, pp. 139–151, 2014.

[5] R. Sansom and G. Strbac, "The impact of future heat demand pathways on the economics of low carbon heating systems," in *BIEE - 9th Academic Conference*, 2012, no. September, p. 10.

[6] S. Heinen, P. Mancarella, C. O'Dwyer, and M. O'Malley, "Heat electrification: The latest research in Europe," *IEEE Power Energy Mag.*, vol. 16, no. 4, pp. 69–78, 2018.

[7] G. Strbac, "Demand side management: Benefits and challenges," *Energy Policy*, vol. 36, no. 12, pp. 4419–4426, 2008.

[8] P. Mancarella and G. Chicco, "Real-time demand response from energy shifting in distributed multi-generation," *IEEE Trans. Smart Grid*, vol. 4, no. 4, pp. 1928–1938, Dec. 2013.

[9] T. Capuder and P. Mancarella, "Techno-economic and environmental modelling and optimization of flexible distributed multi-generation options," *Energy*, vol. 71, pp. 516–533, 2014.

[10] S. Clegg and P. Mancarella, "Integrated electricity-heat-gas network modelling for the evaluation of system resilience to extreme weather," *2017 IEEE Manchester PowerTech, Powertech 2017*, pp. 1–6, 2017.

[11] S. Clegg and P. Mancarella, "Assessment of the impact of heating on integrated gas and electrical network flexibility," *19th Power Syst. Comput. Conf. PSCC 2016*, pp. 1–7, 2016.

[12] S. Clegg and P. Mancarella, "Integrated Electrical and Gas Network Flexibility assessment in Low-Carbon Multi-Energy Systems," *IEEE Trans. Sustain. Energy*, vol. 7, no. NO. 2, pp. 718–731, 2016.

[13] S. Clegg and P. Mancarella, "Integrated electricity-heat-gas modelling and assessment, with applications to the Great Britain system. Part I: High-resolution spatial and temporal heat demand modelling," *Energy*, pp. 1–11, 2018.

[14] S. Clegg and P. Mancarella, "Integrated electricity-heat-gas modelling and assessment, with applications to the Great Britain system. Part II: Transmission network analysis and low carbon technology and resilience case studies," *Energy*, pp. 1–13, 2018.

[15] B. Lu, A. Blakers, M. Stocks, C. Cheng, and A. Nadolny, "A zero-carbon, reliable and affordable energy future in Australia."

[16] N. Good, L. Zhang, A. Navarro-Espinosa, and P. Mancarella, "High resolution modelling of multi-energy domestic demand profiles," *Appl. Energy*, vol. 137, pp. 193–210, 2015.

[17] Australian Energy Market Operator, "2019 Input and Assumptions workbook," 2019.

[18] A. Osiadacz, *Simulation and analysis of gas networks*. 1987.

[19] E. S. Menon, *Gas Pipeline Hydraulics*. 2005.

[20] CSIRO, "Typical House Energy Use - Australian Housing Data," 2013.

[21] Northmore Gordon, "Victorian Gas Market – Demand Side Measures to Avoid Forecast Supply Shortfall," 2020.

[22] Australian Energy Market Operator, "Gas Statement of Opportunities," 2020.

[23] Australian Energy Market Operator, "National Electricity & Gas Forcasting."

[24] Department of Industry Science Energy and Resources, "HVAC factsheet - Boiler efficiency," 2013.

[25] Sustainability Victoria, "Energy Efficiency : Steam , Hot Water and Process Heating Systems," 2010.

[26] Australian Hot Water, "Hot Water Safety."

[27] Bureau of Meteorology, "Climate Data Online." .

[28] Australian Energy Market Operator, "Zonal gas demands." .

[29] Australian Energy Market Operator, "Actual Generation and Load Data." .

[30] Australian Energy Market Operator, "2020 Integrated System Plan database," 2020.

[31] Australian Energy Market Operator, "2020 Integrated System Plan," 2020.

[32] Australian Energy Market Operator, "AEMO ISP 2020 - Renewable Energy Zones Generation Outlook," 2020.

[33] Australian Energy Market Operator, "Western Victoria Renewable Integration PCAR," 2019.

[34] Australian Energy Market Operator, "Technical Guide To the Victorian Declared Wholesale Gas Market," 2013.

[35] Australian Energy Market Operator, "Victorian Gas Planning Report," no. March, 2019.